# Modeling of Micro-Electro-Mechanical Integrated Test Structures

by

SunMan Patrick Wu

Submitted to the Department of Electrical Engineering and Computer Science
in partial fulfillment of the requirements for the degrees of

Bachelor of Science in Electrical Engineering

and

Master of Engineering in Electrical Engineering and Computer Science and Engineering

at the

MASSACHUSETTS INSTITUTE OF TECHNOLOGY

May 1995



Author .....
Department of Electrical Engineering and Computer Science
May 26,1995

Certified by .....
Stephen D. Senturia
Professor
Thesis Supervisor

Accepted by .....
F.R.Morgenthaler
Chairman, Departmental Committee on Graduate Theses

# Modeling of Micro-Electro-Mechanical Integrated Test Structures

by

SunMan Patrick Wu

Submitted to the Department of Electrical Engineering and Computer Science
on May 26,1995, in partial fulfillment of the
requirements for the degrees of
Bachelor of Science in Electrical Engineering
and
Master of Engineering in Electrical Engineering and Computer Science and Engineering

## Abstract

Recently, there has been much work done on Micro-Electro-Mechanical-System (MEMS) structure. A parallel plate capacitor with a movable plate has been proposed in modeling a specific class of structures that exhibit a vertically deflected electrostatic deformation. In this thesis, this capacitor is modeled as a variable capacitor in a differentiator. HSPICE is used to simulate this differentiator,which is used to measure the MEMS capacitance. An input with both DC and AC component are used to stimulate the MEMS circuit and to obtain an output which can be used to measure the MEMS capacitor model. The goal of this thesis is to understand through simulation the effect of the mechanical resonance of the movable plate on the ouput of the measurement circuit.

Thesis Supervisor: Stephen D. Senturia
Title: Professor

# Acknowledgments

I would like to give thanks to King Chung Yu, Zachary Lee, Ernest Yeh, Yitwah Cheung, Warren Lam, Sinyan Law, Brian So, Jimmy Lai, Leo Chun, Kin Lam, Tony Eng, Andy Tang, and Jeffrey Kim for all their encouragement, and advice throughout the time of writing up this thesis. Special thank to professor Stephen Senturia, Raj Rupta, and G.K. Anathasuresh for their technical help and their patience in teaching me things for this project. This work was supported by ARPA(Contract J-FBI-92-196). Also, I would like to express my gratitute to my parents for their support throughout my five years in MIT. Finally, I thank my LORD for HIS love on me and HIS guidance as HE always provide the best thing for me.

# Contents

# List of Figures

# List of Tables

# Chapter 1

# Introduction

As the technology of micromechanical structure arised during this past half decade, this recent development have been implemented onto the integrated chips for more engineering applications.[1]. Currently, the MIT Microsystem Technology Laboratory MEMCAD research group is cooperating with Analog Devices in designing a chip using the iMEMS process. The iMEMS process integrates micromechanical test structures with other electronics components within the chip, facilitating the observation and recording of any kind of structural deformations when electrical stimuli are applied to these test structures. This chip contains test structures(a mechanical component), a resistor, and an operational amplifier(electrical components); all together they make up a differentiator. Thus, the chip can be considered a Micro-Electro-Mechanical System(MEMS) structure.

## 1.1 Objective of MEMS Structures Modeling

The objective of this project is to simulate a model for MEMS structures in order to gain a better understanding of how these structures behave. We focus on structures which have vertically deflected deformations. Three such structures are the cantilever, the fixed-fixed beam, and the clamped circular diaphragm.Figures 1-1.

## 1.2 Organization

This thesis is organized in the following manner. Chapter 2 describes a conceptual model for MEMS structures. Chapter 3 presents the circuit model of the test characterization chip which involves translating the mechanical conceptual model into an equivalent electrical circuit model which is suitable for HSPICE simulation. Finally Chapter 4 concludes with a discussion of the HSPICE simulation results.

# Examples of the Vertical Deflected Electrostatic Deformation MEMS Structures

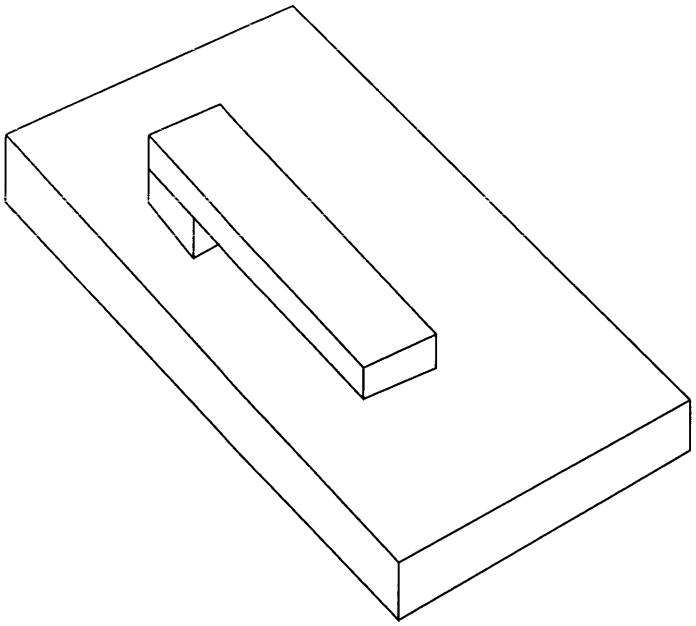

A) the Cantilever Beam(Side View)

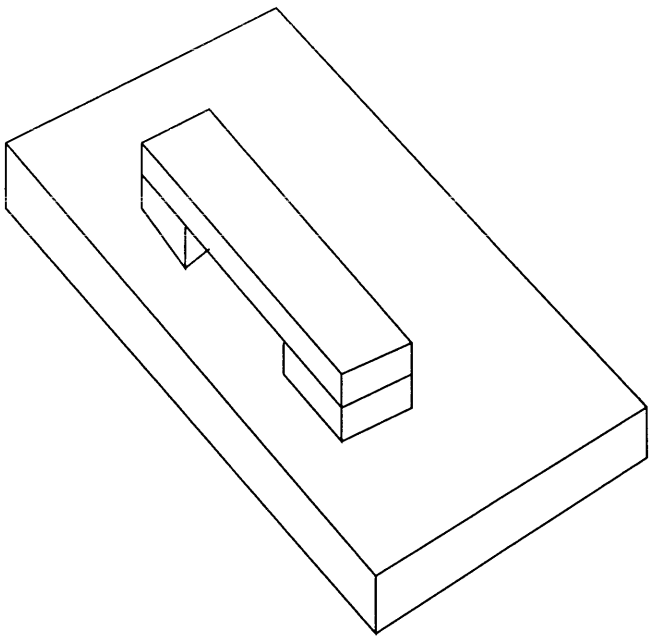

B) the Fixed-Fixed Beam (Side View)

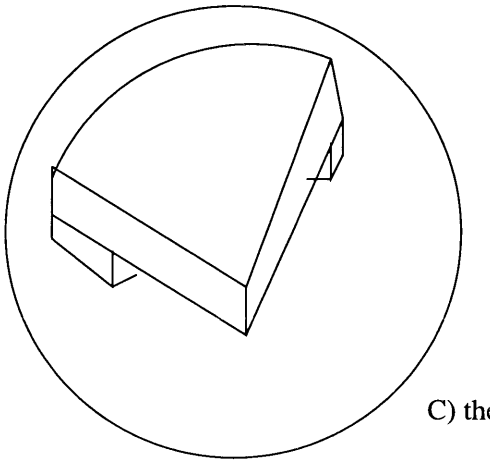

C) the Clamped Circular Diaphragm(cut-away view)

Figure 1-1: Vertically Deflected Electrostatic Deformated MEMS Structures.

# Chapter 2

# Background

## 2.1 Description of the Conceptual Model

We are interested in modeling the class of MEMS structures that exhibits electrostatic, vertically deflected deformations. When a load is applied to MEMS structures, the MEMS structures start bending and deforming differently, each according to its unique mechanical properties. However, once this load is removed, the MEMS structures' intrinsic compliance allows them to restore themselves back to their original shapes. But if the applied load exceeds a certain threshold, the system becomes unstable. At that point, the load no longer controls the bending of the beam, and the beam will bend to the ground, a phenomenon called Pull-In. A conceptual model was formulated in [2] to predict the range of possible behavior of these structures. The model, shown in Figure 2-1, consists of a parallel-plate capacitor attached to a mechanical spring. One plate of the capacitor is physically fixed while the other plate is held suspended by an ideal linear mechanical spring. The spring is modeled by its spring constant. The model is made assuming no fringing field effect.

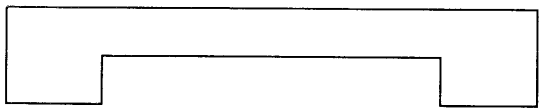

Figure 2a: fixed-fixed beam without any load

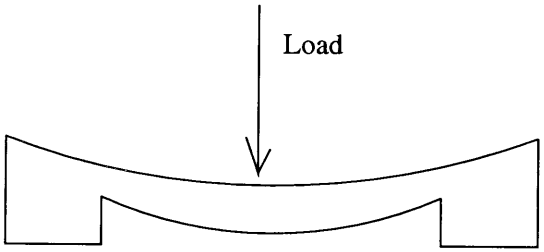


Figure 2b: the vertical deflection bending of the fixed-fixed beam under a load

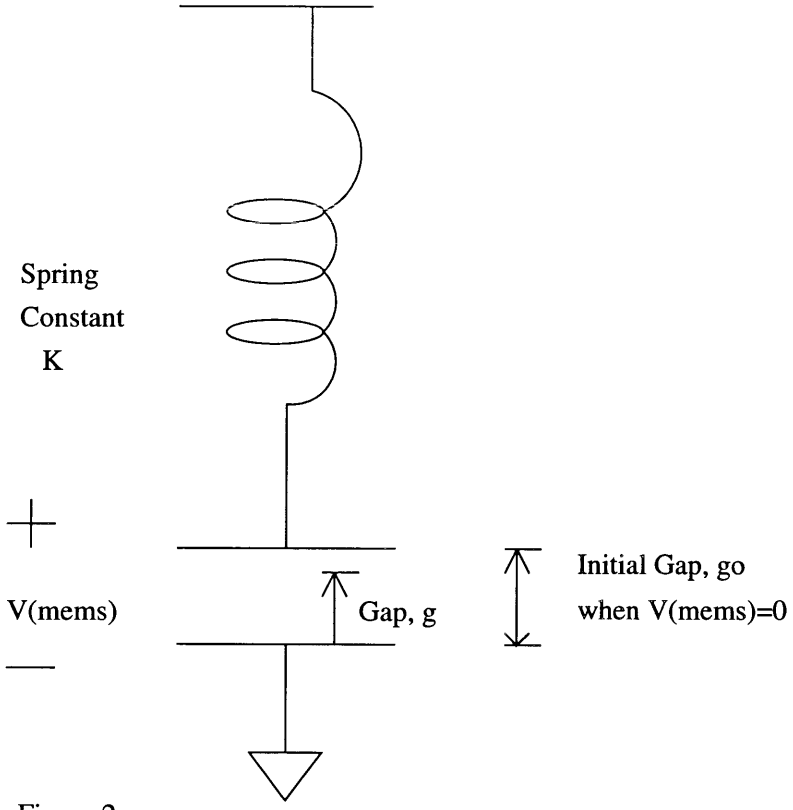


Figure 2.
Lumped Parallel-Plate Capacitor Conceptual Model of the MEMS Structure

Figure 2-1: MEMS Conceptual Mechanical Models and Dynamic Behavior Description.

Initially, when there is no voltage applied to the model, there is an initial gap, $g_0$, which represents the physical distance between the capacitor plates. Once a voltage is applied, charge starts to build up on the plates and in this manner engery is stored within the capacitor. The top plate of the capacitor begins to pull down due to force generated by the electric field across the capacitor plates. Thus, a displacement $x$ occurs. The distance, g, between the capacitor at any given input voltage is given by:

$$g(V_{in}) = g_0 - x(V_{in}) \tag{2.1}$$

The MEMS capacitance is a function of the displacement $x$:

$$C(V_{in}) = \frac{\epsilon_o A}{g(V_{in})} = \frac{\epsilon_o A}{g_0 - x(V_{in})} \tag{2.2}$$

where both g and x are functions of $V_{in}$, the input voltage applied on the capacitor. In this model, the voltage $V_{in}$ and displacement $x$ are analogous to the load and the amount of bending of MEMS structures respectively. At equilibrium, the force of the spring is equal to the negative gradient of the energy of the capacitor in the system. Thus, the force balance equation can be written as:

$$K\left(g_o - g\right) = Kx = -\frac{d}{dx}\left(\frac{1}{2}C{V_{in}}^2\right) = \frac{\epsilon_o A {V_{IN}}^2}{2\left(g_o - x\right)^2} \tag{2.3}$$

In this model, the displacement $x$ increases along with the magnitude of the applied voltage. But once the voltage reaches a certain threshold, which we called the $pull-in$ voltage, the model becomes unstable and the top plate of the capacitor simply collapses onto the ground plate. In order to find out when the pull-in incident occurs, we compute the saddle point value of the total energy of the system by finding the second derivative with respect to $x$. This is equivalent to taking $\frac{d}{dx}$ on both side of Equation 2.3. Here, we get:

$$K = \frac{\epsilon_o A {V_{in}}^2}{\left(g_o - x\right)^3} \tag{2.4}$$

Substituting K into Equation 2.3, we have:

$$\frac{\epsilon_o A {V_{in}}^2}{2x\left(g_o - x\right)^2} = \frac{\epsilon_o A {V_{in}}^2}{\left(g_o - x\right)^3} \tag{2.5}$$

After some cancellation of terms on both sides, we have $g_0 - x = 2x$, which implies that $g_0 = 3x$, $g = g_0 - x = 2x$, and thus

$$g = \frac{2g_0}{3} \tag{2.6}$$

This means that when the displacement reaches $\frac{1}{3}$ of the initial gap length, the model becomes unstable and causes Pull-In. Thus, from Equation 2.3 and 2.6, we can derive the Pull-In voltage as

$$V_{PI} = \sqrt{\frac{8K{g_0}^3}{27\epsilon A}} \tag{2.7}$$

The following are some realistic values for the some of parameters: K=164N/m, $g_0$=1.6um, A=50$\mu$m $x = 500\mu m$, $\epsilon_o = 8.85 \times 10^{-12}$F/m. The Pull-In voltage comes out to be approximately $V_{PI} = 30$ Volts. Therefore, we require that the input voltage be less than the Pull-In voltage to ensure stability in this model. One can describe the displacement of the capacitor using the following second order differential equation:

$$M\frac{d^2x}{dt^2} + b\frac{dx}{dt} + Kx = F_{ext} = \frac{{V_{IN}}^2 \epsilon_o A}{2\left(g_o - x\right)^2} \tag{2.8}$$

where the mass of the silicon material, M= 1.1655e-10kg, and the damping factor b= $10^{-10}$.

When voltage is applied onto the capacitor, the top plate begins to move and to oscillate until it reaches a steady state due to the effect of the damping factor. This concludes the general description of the 1-D parallel plate capacitor model.

# Chapter 3

# Implementation

The capacitor model is merely an abstraction of MEMS structures. It only provides an approximation and a closed-form expression for the pull-in voltage based on parameters like the spring constant, the capacitor gap and area. In order to use the conceptual model for electrical engineering purposes, Raj Gupta has designed a material characterization chip using Analog Device's iMEMS process. This is a differentiator chip with a resistor, an operational amplifier, and vertical deflected electrostatic micromechancial structures. As described in Chapter 1, this iMEMS process integrates MEMS structures with other electronic components within a chip. This process allows the MEMS structures to interact with other electronics part. Thus, all kinds of mechanical deformations can be observed and translated to electrical output signals of the chip. The objective of this project is to simulate the test characterizations of the chip using the HSPICE program by modeling MEMS using electrical circuit models. The conceptual model of the MEMS structure is modeled by a electrical analogy of a variable capacitor with a function described by Equation 2.2. To obtain the displacement $x$ of the capacitor plate, the mechanical second order differential equation governing this model must be translated into a corresponding electrical model for use in HSPICE simulation. This mechanical differential equation relates force to velocity as state variables. Figure 3-1 shows the overall configuration of the circuit in this simulation. The circuit consists of a differentiator that has a MEMS capacitor and two displacement RLC circuits which determine the amount of

| Mechanical Domain | Electrical Domain |
|---|---|
| $F_b = \mathrm{b}\ v$ | $V_R = \mathrm{R\ I}$ |
| $F_M = \mathrm{M}\ \frac{dv}{dt}$ | $V_L = \mathrm{L}\ \frac{dI_L}{dt}$ |
| $F_K = \mathrm{K} \int v_K dt$ | $V_C = \frac{1}{C} \int I_C dt$ |

Table 3.1: Analogy between Mechanical and Electrical State Variables.

DC and AC displacements observed in the MEMS capacitor plates.

In designing the displacement RLC circuits, the differential equation from the mechanical domain must be translated into an electrical analogue since only electrical circuits can be simulated by HSPICE. One can make an analogy between force and voltage as "across" variables in their respective domain, and similiarly between velocity and current as "through" variables. Table 3.1 compares the mechanical and electrical domains of these state variables.

Using this mapping, the second order differential equation can be modeled by a RLC circuit. The output of this RLC circuit determines the displacement $x$ of the MEMS capacitor from the differentiator. The resistance is set to be the damping factor, R = b. The inductor has the mass value, L= M and the capacitor is related to the spring constant as C= $\frac{1}{k}$. The input of the RLC circuit is in the form of a voltage dependent source based on the external force $F_{ext}$ described by Equation 2.8.

$$F_{ext} = -\nabla\left(\frac{C_{MEMS}{V_{in}}^2}{2}\right) = \frac{\epsilon_o A {V_{in}}^2}{2\left(g_0 - \left(X_{DC} + X_{AC}\right)\right)^2} = \frac{\epsilon_o A {V_{in}}^2}{2\left(g_0 - \left(\frac{V_{XDC}+V_{XAC}}{K}\right)\right)^2} \tag{3.1}$$

The following equation is based on the MEMS capacitance given by an expanded version of Equation 2.2.

$$C_{MEMS}\left[V_{IN}\left(t\right)\right] = \frac{\epsilon_o A}{\left(g_0 - \left(X_{DC}\left[V_{IN}\left(t\right)\right] + X_{AC}\left[V_{IN}\left(t\right)\right]\right)\right)} = \frac{\epsilon_o A}{\left(g_0 - \left(\frac{V_{XDC}[V_{IN}(t)]+V_{XAC}[V_{IN}(t)]}{k}\right)\right)} \tag{3.2}$$

where $V_{XDC}$, $V_{XAC}$, $X_{DC}$, and $X_{AC}$ are functions of the input voltage $V_{IN}\ (t)$

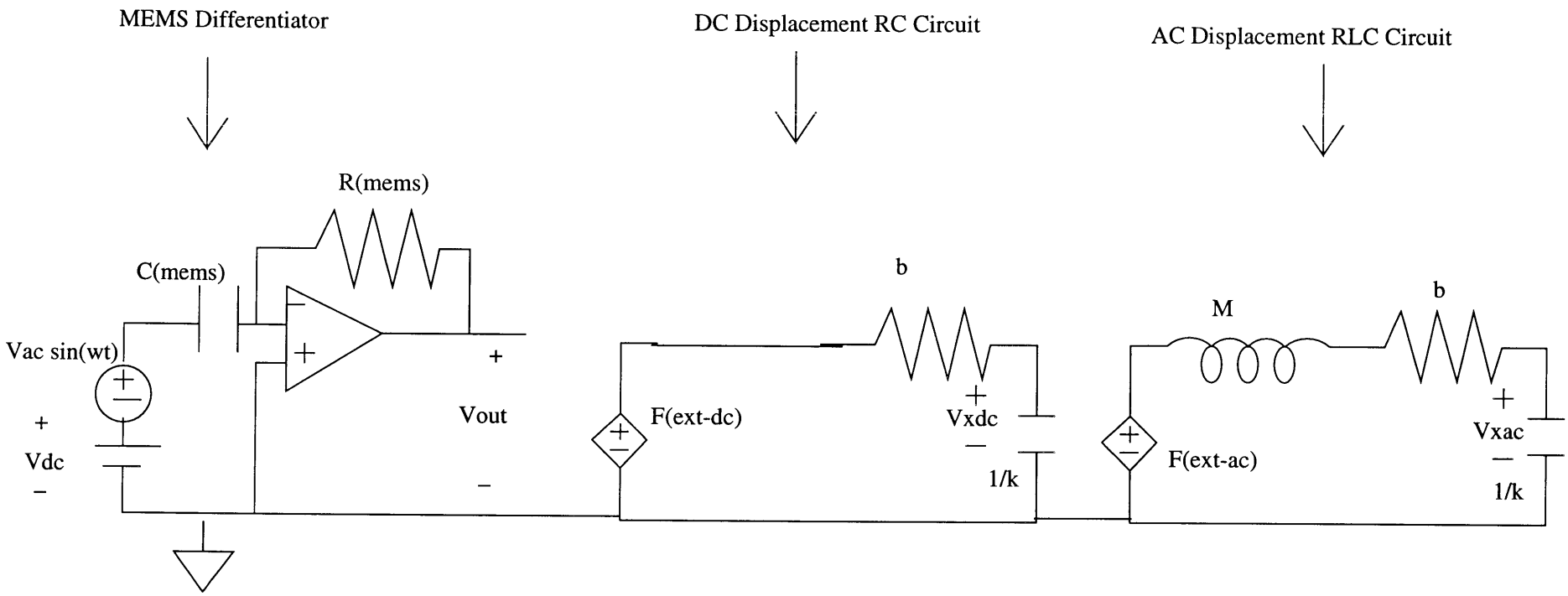


Figure 3-1: MEMS Structure Simulated Circuit Schematics

while $X_{DC}$= $\frac{V_{XDC}}{k}$ and $X_{AC}$= $\frac{V_{XAC}}{k}$. The external force dependent source $F_{ext}$ is a function of the input voltage $V_{IN}$ and its own displacement feedback voltages,$V_{XDC}$ and $V_{XAC}$. $V_{XDC}$ and $V_{XAC}$ determine $C_{MEMS}$, the MEMS capacitance. For the differentiator, our objective is to study its steady state capacitance in the MEMS structure. However, since this is a differentiator, in order to make any measurement of capacitance on the output voltage, it is necessary to include both the DC and AC components on the input voltage. But by adding the AC component, the system is perturbed in the following manner. The DC and AC parts of input voltage generates their corresponding displacement voltages $V_{XDC}$ and $V_{XAC}$ respectively on the two displacement circuits. The two displacement voltages causes the MEMS capacitance to have both the DC and AC components from Equation 3.2. The objective of this thesis is to figure out how significant this perturbation is and to measure the DC steady state MEMS capacitance. In general, the AC component should be insignificant compared to the DC component for a wide range of frequencies that drives the differentiator. However, the AC component is much more significant when the differentiator is driven by an input at the resonant frequency of the RLC circuit. At this frequency, the AC component output of the RLC circuit becomes much greater than usual and contributes a larger amount of perturbation to the calculation of the MEMS capacitance of the differentiator. Results of the RLC outputs driven at different frequencies are presented in Chapter 4. Since our goal is to separate the DC from the AC components of the input, two RLC displacement circuits are used to generate the $V_{XDC}$ and $V_{XAC}$ separately. If $V_{DC}$ and $V_{AC}$ are magnitudes of the DC and AC inputs, and $w_d$ is the driving frequency of the differentiator, we have that

$$V_{IN} = V_{DC} + V_{AC} \sin(w_d t) \tag{3.3}$$

Thus,

$$V_{IN}{}^2 = V_{DC}{}^2 + 2V_{DC}V_{AC} \sin(w_d t) + V_{AC}{}^2 \sin^2(w_d t) \tag{3.4}$$

Using the identity,

$$\sin^2(w_d t) = \frac{1 - \cos(2w_d t)}{2} \tag{3.5}$$

we can write Equation 3.4 as

$$V_{IN}{}^2 = V_{DC}{}^2 + \frac{V_{AC}^2}{2} + 2V_{DC}V_{AC}\sin(w_d t) - \frac{V_{AC}{}^2\cos(2w_d t)}{2} \tag{3.6}$$

The first two terms of Equation 3.6 form the DC component input and the last two terms make up the AC component input. The DC component depends only on the magnitude of $V_{DC}$ and $V_{AC}$. The AC component depends on $V_{AC}$, and both the driving frequency and its double frequency, $w_d$ and $2w_d$

## 3.1 Taylor Series Approximation for HSPICE

In simulating the circuit into HSPICE file format, problems arose since HSPICE can only take polynomial function for the dependent voltage source in the RLC circuits.[3] But $F_{ext}$ (see Equation 3.1) is not in the form of a polynomial but in the form of complex fraction, with dependent voltages on both the denominator and numerator. To overcome this limitation, a Taylor Series Approximation was used to expand the fraction into a series with finite terms. However, since we approximated the series and threw out the higher order terms, some tolerance testing was done in predicting the accuracy of the model used. Below is the series:

$$\frac{1}{(g_0 - V_x k)^2} = \frac{1}{g_0^2}\left(1 + \frac{2V_x}{g_0 k} + 3\left(\frac{V_x}{g_0 k}\right)^2 + .....\right) \tag{3.7}$$

In the DC displacement RLC circuit, since the input is in the form of pure DC source, there is no frequency component driving this circuit. To facilitate the analysis, given the small inductance from a mass value of 1.1655e-10 kg, it is reasonable to assume that the inductor acts liked a short circuit as most current passes through without significantly dropping the voltage across it. However, the inductor can't be ignored in the AC displacement circuit since it has a frequency dependent input. Thus, we

can write the DC and AC components of the external force as:

$$F_{ext-dc} = \frac{\epsilon_o A}{2g_0^2}\left(V_{DC}^2 + \frac{V_{AC}^2}{2}\right)\left(1 + \frac{2V_{xdc}}{g_0 k} + 3\left(\frac{V_{xdc}}{g_0 k}\right)^2 + .....\right) \tag{3.8}$$

$$F_{ext-ac} = \frac{\epsilon_o A}{2g_0^2}\left(2V_{DC}V_{AC}\sin(w_d t) - \frac{{V_{AC}}^2\cos(2w_d t)}{2}\right)\left(1 + \frac{2V_{xac}}{g_0 k} + 3\left(\frac{V_{xac}}{g_0 k}\right)^2 + .....\right) \tag{3.9}$$

Since the Taylor series approximation is used by HSPICE, it is necessary to check the accuracy of the approximation with a range numbers of terms used. The MEMS capacitance was derived analytically and compared with simulation results for tolerance testing. From Equation 2.3, we have

$$Kx = \frac{\epsilon_o A {V_{in}}^2}{2(g_0 - x)^2} = \frac{(C_{MEMS}V_{IN})^2}{2\epsilon_o A} \tag{3.10}$$

Solving for $x$ from Equation 2.2 as a function of $C_{MEMS}$, we get:

$$x = g_0 - \frac{\epsilon_o A}{C_{MEMS}} \tag{3.11}$$

Substitute $x$ in Equation 3.10, we get the following third degree polynomial relating $C_{MEMS}$ and $V_{in}$:

$$\left(\frac{{V_{in}}^2}{2\epsilon_o k A}\right)C_{MEMS}^3 - g_0 C_{MEMS} + \epsilon_o A = 0. \tag{3.12}$$

Matlab was used to solve this third order polynomial in this implicit form. The output graph of this Matlab program is attached on Figure 3-2. In this program, we ploted $\frac{1}{C}$ vs. $V_{IN}^2$ with $V_{IN}$ ranging from 0 V to $V_{PI}$= 30 V so that $V_{IN}^2$ is between 0 and 900 $volts^2$. Given a specific value of $V_{IN}$, there are 3 roots values of C. However, two of the three roots are complex conjugates and can be ignored. The real root is the root of interest and the corresponding $\frac{1}{C}$ value is calculated from it.

HSPICE simulations with three terms of the Taylor series approximation were also simulated with $V_{IN}^2 = V_{DC}^2 + \frac{1}{2}V_{AC}^2$. $V_{AC}$ was fixed to 0.5 volts while $V_{DC}$ was varied in order to generate a range of values for $V_{IN}^2$ from 0 to 900 $volts^2$. The AC

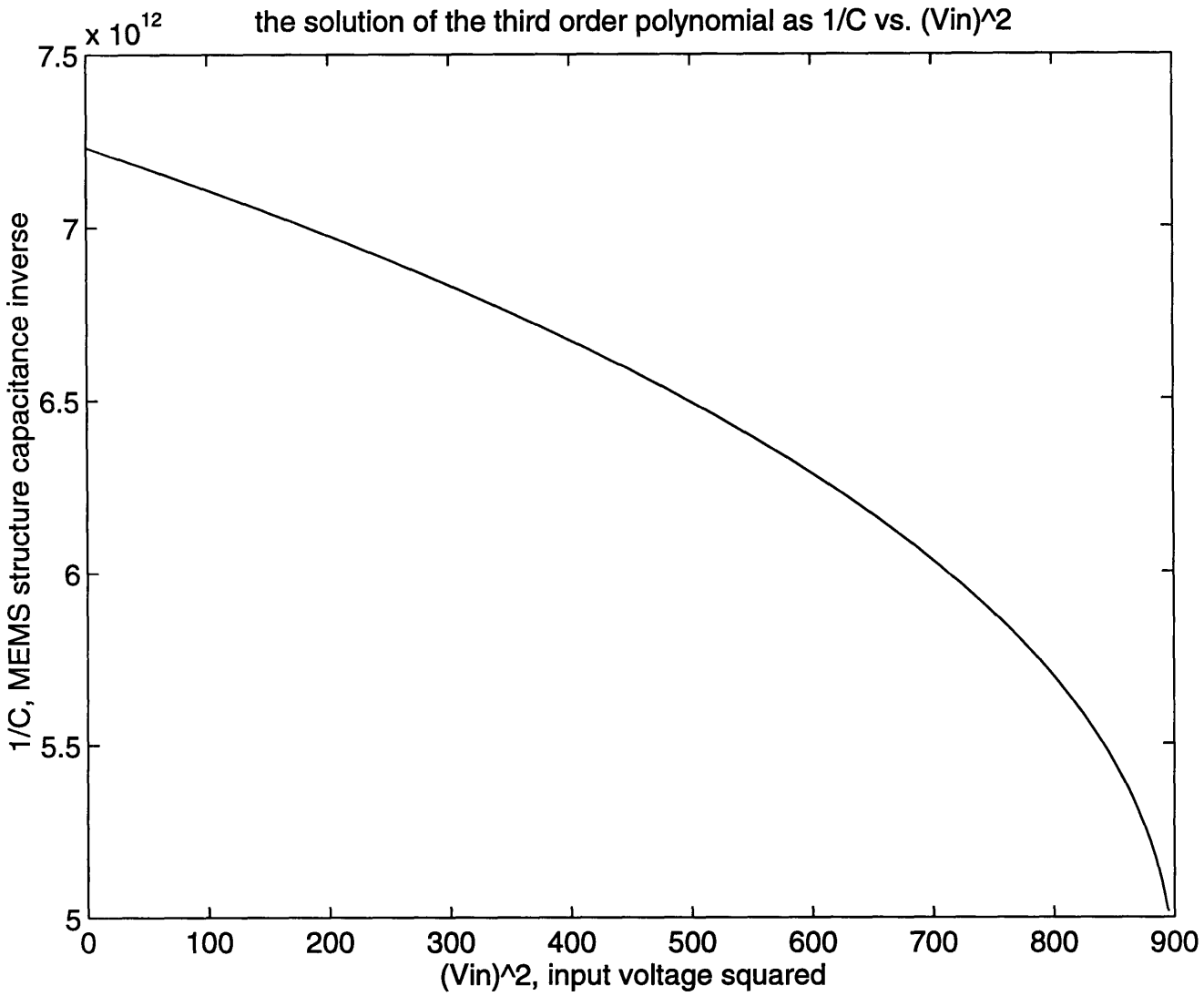


Figure 3-2: Matlab Solution for the third degree Polynomial in $\frac{1}{C}$ vs. $V_{in}^2$

| $V_{IN}^2$ | $V_{XDC}$ $(volt)$ | $C_{HSPICE} = \frac{\epsilon_0 A}{g_0 - \frac{V_{XDC}}{k}}$ $(Farad)$ | $C_{MATLAB}$ | Percentage error |
|---|---|---|---|---|
| 25 | 2.1917e-6 | 1.3946e-13 | 1.38859e-13 | 0.431% |
| 36 | 3.1826e-6 | 1.39979e-13 | 1.3909367e-13 | 0.88533% |
| 50 | 4.4666e-6 | 1.40675e-13 | 1.394506e-13 | 0.87037% |
| 55 | 4.9315e-6 | 1.40929e-13 | 1.395712e-13 | 0.96346% |
| 60 | 5.3999e-6 | 1.41187e-13 | 1.3969212e-13 | 1.0588% |
| 65 | 5.8719e-6 | 1.41446e-13 | 1.398132e-13 | 1.15436% |

Table 3.2: Percentage Error of MEMS Capacitance

component of the displacement RLC circuit , $V_{XAC}$ is ignored in this analysis since we are only interested in the steady state capacitance, which depend only on the $V_{XDC}$. Once the displacement voltage was obtained from the simulation given a $V_{IN}^2$; The resulting $V_{XDC}$ from simulated is used to determine the $C_{MEMS}$ from Equation 2.2. This result is compared to the capacitance value solved by Matlab. In Table 4.1, the two capacitance values are compared and the percentage error of $C_{MEMS}$ with respect to $C_{MATLAB}$ is computed. For this simulation, we require that the results fall within 99 percents accuracy or one percent tolerance; This condition is satisfied as long as the input voltage do not exceed 7.4 volts or $V_{IN}^2 = 55\ volts^2$. This has found to be true regardless of taking the first one, two or three terms of the Taylor Series for approximation. Thus, it is decided to use $V_{DC}$=5 volts and $V_{AC}$=.5 volt for the simulation of the circuit in HSPICE, a value which is below the 7.4 volts, or $V_{IN}^2$=55 $volts^2$ limit. We use three terms for Taylor Series approximation. The HSPICE input file is listed in Appendix A.

The differentiator circuit has a nonlinear MEMS capacitor. Using KCL (Kirchoff Current Law), we can relate the input current the output current. At the node connected to the negative input of the operational amplifier, we have

$$I = \frac{dQ}{dt} = \frac{d}{dt}\left(V_{IN}C_{MEMS}\right) = C\frac{dV_{IN}}{dt} + V_{IN}\frac{dC_{MEMS}}{dt} = \frac{-V_{out}}{R} \tag{3.13}$$

Taking the derivative of Equation 3-2, we have

$$\frac{dC_{MEMS}}{dt} = \frac{\epsilon_o A}{k\left[g_0 - \left(\frac{V_{XDC}+V_{XAC}}{k}\right)\right]^2}\left(\frac{dV_{XAC}}{dt}\right) = \frac{C_{MEMS}}{k\left(g_0 - \left(\frac{V_{XDC}+V_{XAC}}{k}\right)\right)}\left(\frac{dV_{XAC}}{dt}\right) \tag{3.14}$$

This assumes that $\frac{dV_{XDC}}{dt} = 0$ since $V_{XDC}$ reaches a constant value at a steady state.

Since $V_{IN} = V_{DC} + V_{AC}\sin w_d t$, we can calculate $V_{OUT}$ as:

$$-V_{OUT} = RC_{MEMS}\frac{d}{dt}(V_{DC} + V_{AC}\sin w_d t) + (V_{DC} + V_{AC}\sin w_d t)\left[\frac{RC_{MEMS}}{k\left(g_0 - \left(\frac{V_{XDC}+V_{XAC}}{k}\right)\right)}\left(\frac{dV_{XAC}}{dt}\right)\right] \tag{3.15}$$

$$-V_{OUT} = w_d RC_{MEMS}V_{AC}\cos w_d t + (V_{DC} + V_{AC}\sin w_d t)\left[\frac{RC_{MEMS}}{k\left(g_0 - \left(\frac{V_{XDC}+V_{XAC}}{k}\right)\right)}\left(\frac{dV_{XAC}}{dt}\right)\right] \tag{3.16}$$

This output voltage consists of a sum of two product terms. The first product term is the steady state output. The second big product term is due to the changing $C_{MEMS}$ values since $V_{XAC}$ varies as a function of time. It is this second product term which causes the perturbation when measuring the output of the differentiator.

# Chapter 4

# Results and Discussion

HSPICE simulations have been made for various frequencies for the whole circuit(see Figure 3-1). Results of the various graphs are plotted on Figure 4-1 to 4-7. One of the main goals of this project was to determine both the DC and AC components of the displacement RLC circuit outputs at various frequencies. These two displacement voltages would determine both the DC and AC parts of the MEMS capacitance which in turn determine the total output of the differentiator voltage. Three frequencies, $\frac{w_0}{10}$, $w_0$ and $10w_0$ are used in the simulation where $w_0$ is the natural frequency of the RLC circuit. The resonant frequency of a RLC circuit is:

$$w_o = \sqrt{\frac{1}{LC} - \frac{R^2}{2L^2}} = \sqrt{\frac{k}{M} - \frac{b^2}{2M^2}} \tag{4.1}$$

In the simulation, we drive the circuit with an input of $V_{DC}$ = 5 V and $V_{AC}$= 0.5 V. The DC displacement voltage generated from the displacement RLC circuit is $V_{XDC}$ = 2.2 $\mu$volt, independent of the frequency driving the circuit. Figures $4-1$, $4-2$, and $4-3$ show the AC displacement voltage $V_{XAC}$ at $10w_0$, $w_0$, and $0.1w_0$ respectively. In Figure $4-1$, when the circuit is driven with a very high frequency of $10w_0$, the output $V_{XAC}$ shows a sinusoidal decaying output; it decays from 22 nano-volts to a steady sinusoidal output of 2.2 nano-volt within 120 $\mu$s. When the circuit is driven by a small frequency ($0.1w_0$), the ouput reaches a steady sinusoidal output of 225 nano-volts within 75 $\mu$s(see Figure 4-3). However, when the MEMS differentiator

circuit is driven by the natural frequency $w_0$ of the displacement RLC circuit, $V_{XAC}$ reaches an output of 2.98 $\mu$V in 100 $\mu$s(see Figure 4-2). At this frequency, $V_{XAC}$ is no longer negligible compared to $V_{XDC}$. According to Equation 3.2, this does have a great impact in changing the MEMS capacitance of the circuit. Figure 4-4 shows the three $V_{XAC}$ driven by the three frequencies together along with the $V_{XDC}$; this just indicates the relative differences in magnitude between the three $V_{XAC}$ and the $V_{XDC}$. The three different $V_{OUT}$ vs. $V_{IN}$ graphs at the three different frequencies are plotted in Figure 4-5 to 4-7. In all three graphs, $V_{IN} = 5 + 0.5\sin w_d t$. In Figure 4-5, when the circuit is driven by $w_d$=$10w_o$, $V_{OUT}$ has a magnitude of 11.6574 volts, a value which is much greater than the input voltage. In Figure 4-6, the circuit is driven by a frequency of $w_o$, the output has a magnitude of 1.16 volts, about $\frac{1}{10}$ the magnitude of the output when driven by $10w_o$. Finally, in Figure 4-7, when driven by $0.1w_o$, the output voltage has a magnitude of 0.11 volts, which is $\frac{1}{10}$ of the output of the circuit when driven by $w_o$. The output voltages are approximately linearly proportional to the driving frequency of the circuit, which is expected for a differentiator.

FIGURE 4-1: AC DISPLACEMENT VOLTAGE, VXAC VS. TIME WHEN WD-10WO.

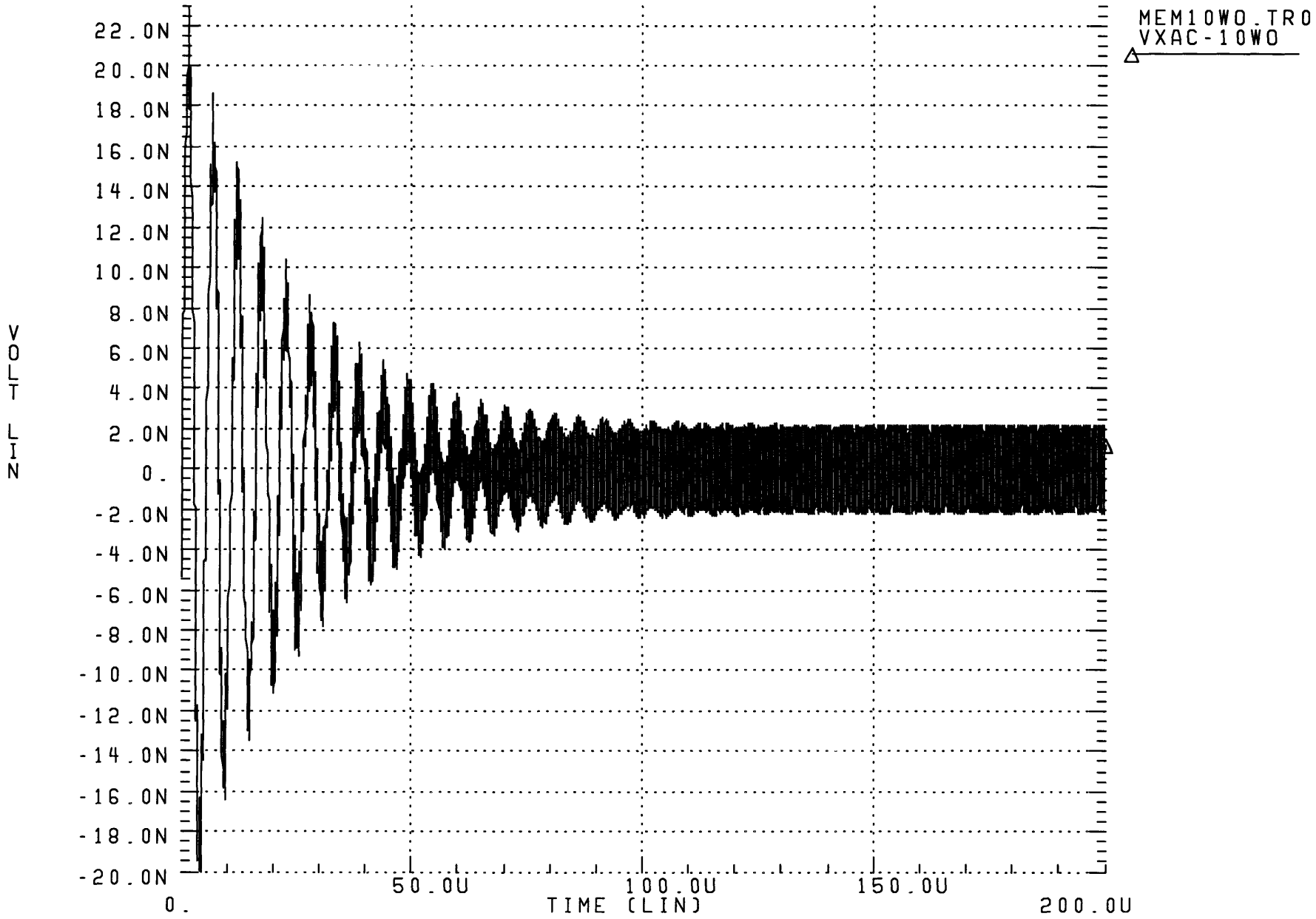

FIGURE 4-2: AC DISPLACEMENT VOLTAGE, VXAC VS. TIME WHEN WD=WO.

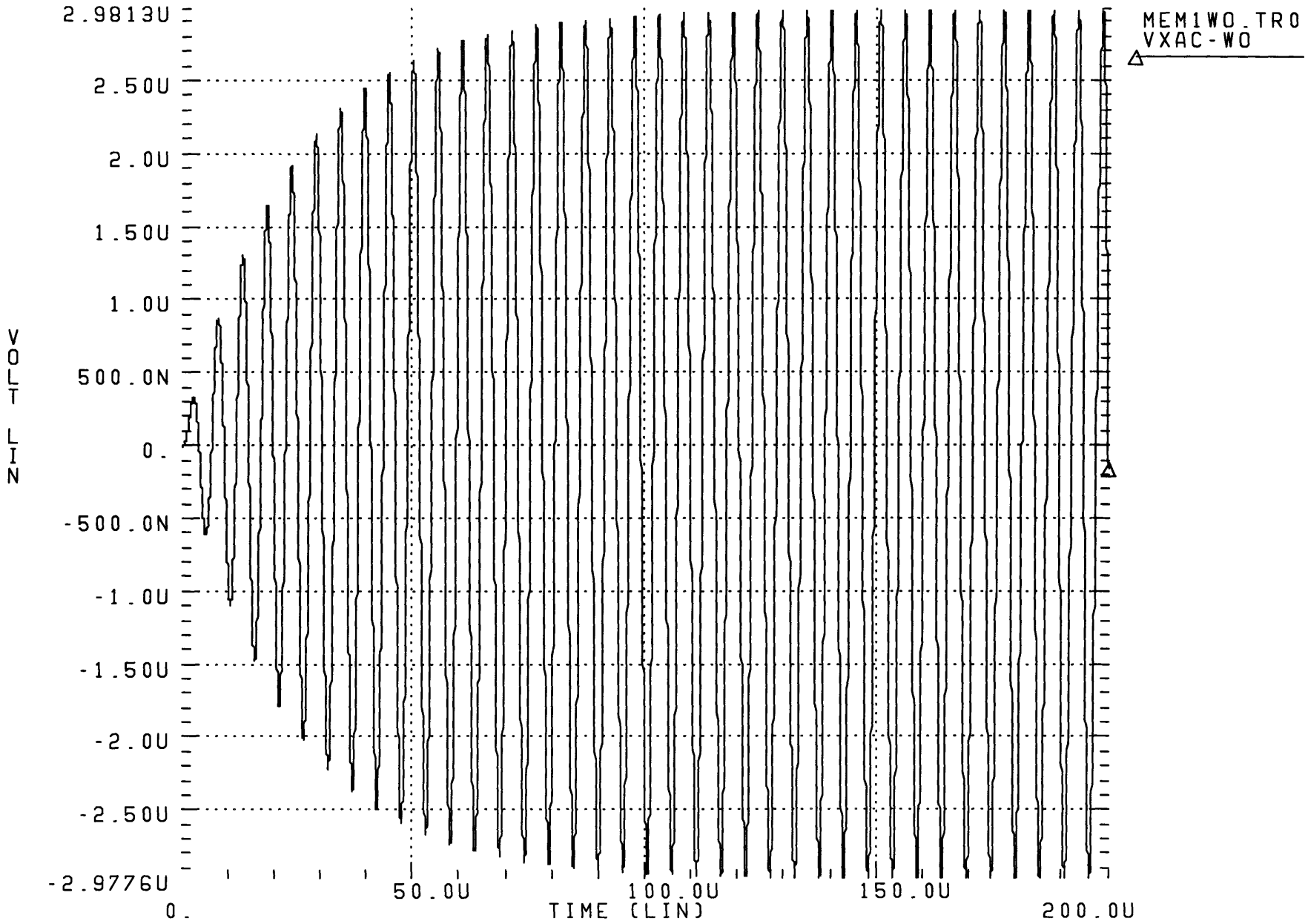

FIGURE 4-3: AC DISPLACEMENT VOLTAGE, VXAC VS. TIME WD=0.1WO.

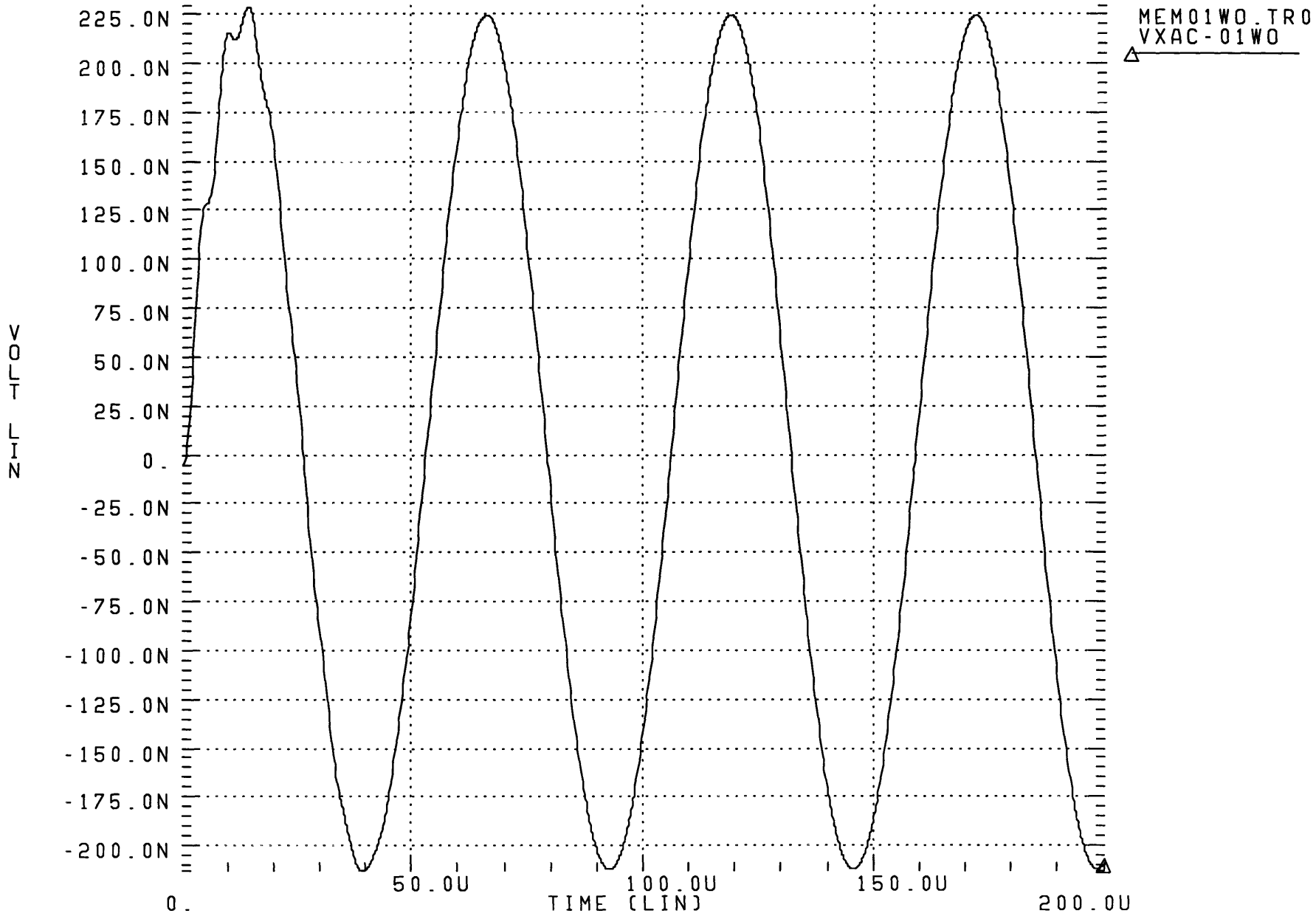

FIGURE 4-4: VXDC AND THE 3 DIFFERENT VXAC DRIVEN BY WD= 0.1WO, WO AND 10 WO.

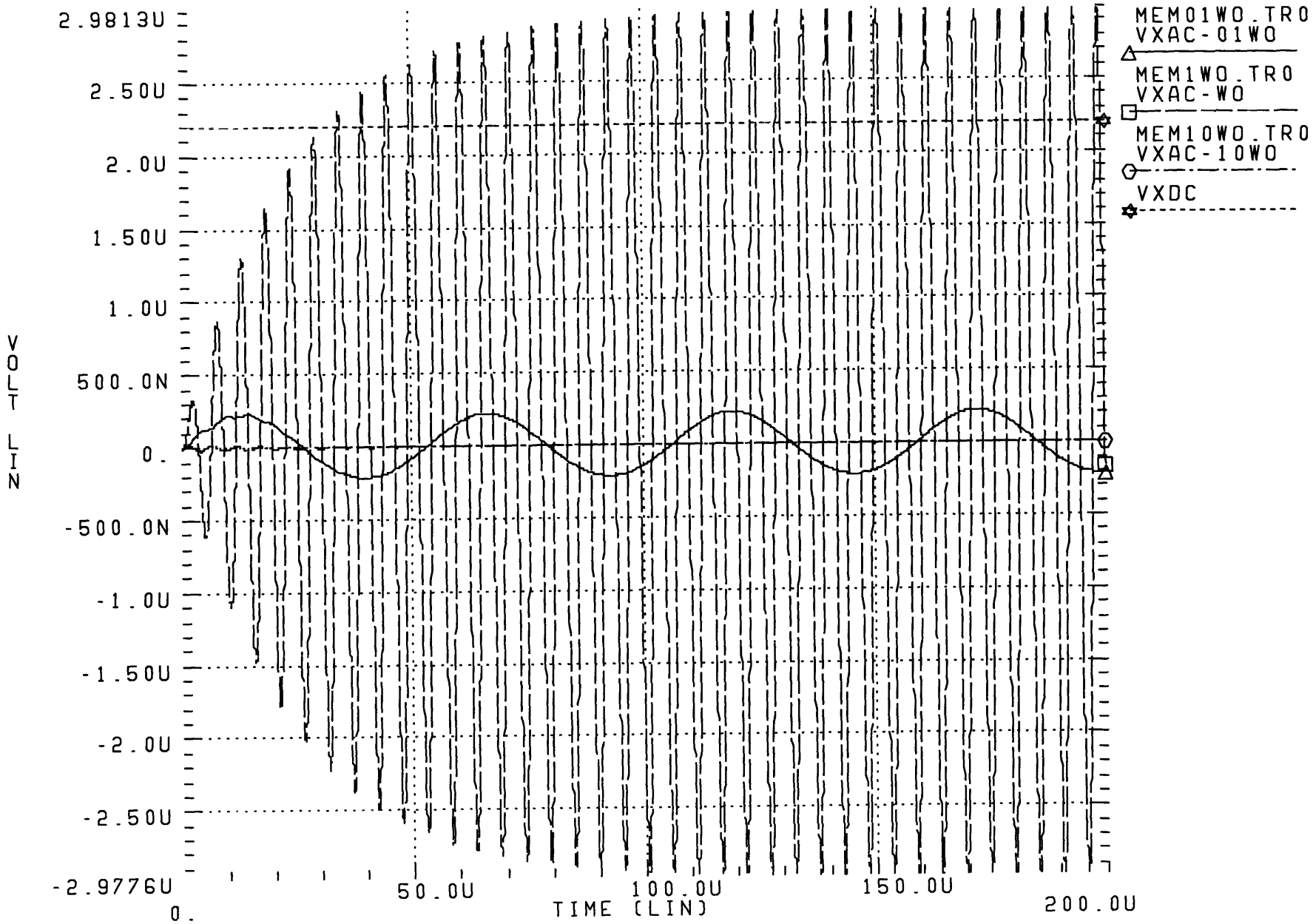

FIGURE 4-5: VOUT AND VIN OF THE WHOLE CIRCUIT VS. TIME, DRIVEN BY WD-10 WO

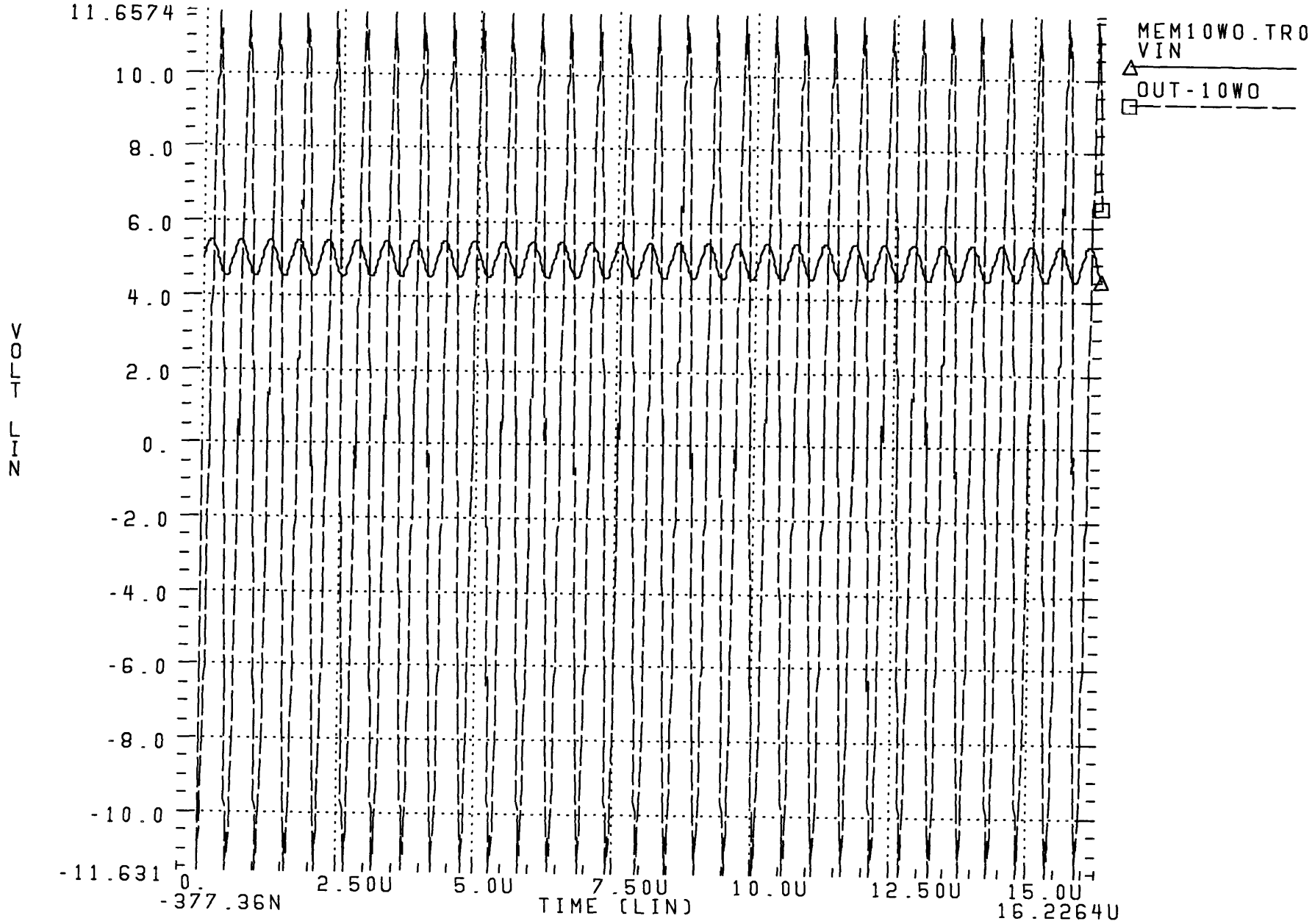

FIGURE 4-6: VOUT AND VIN OF THE WHOLE CIRCUIT VS. TIME, DRIVEN BY WD-WO

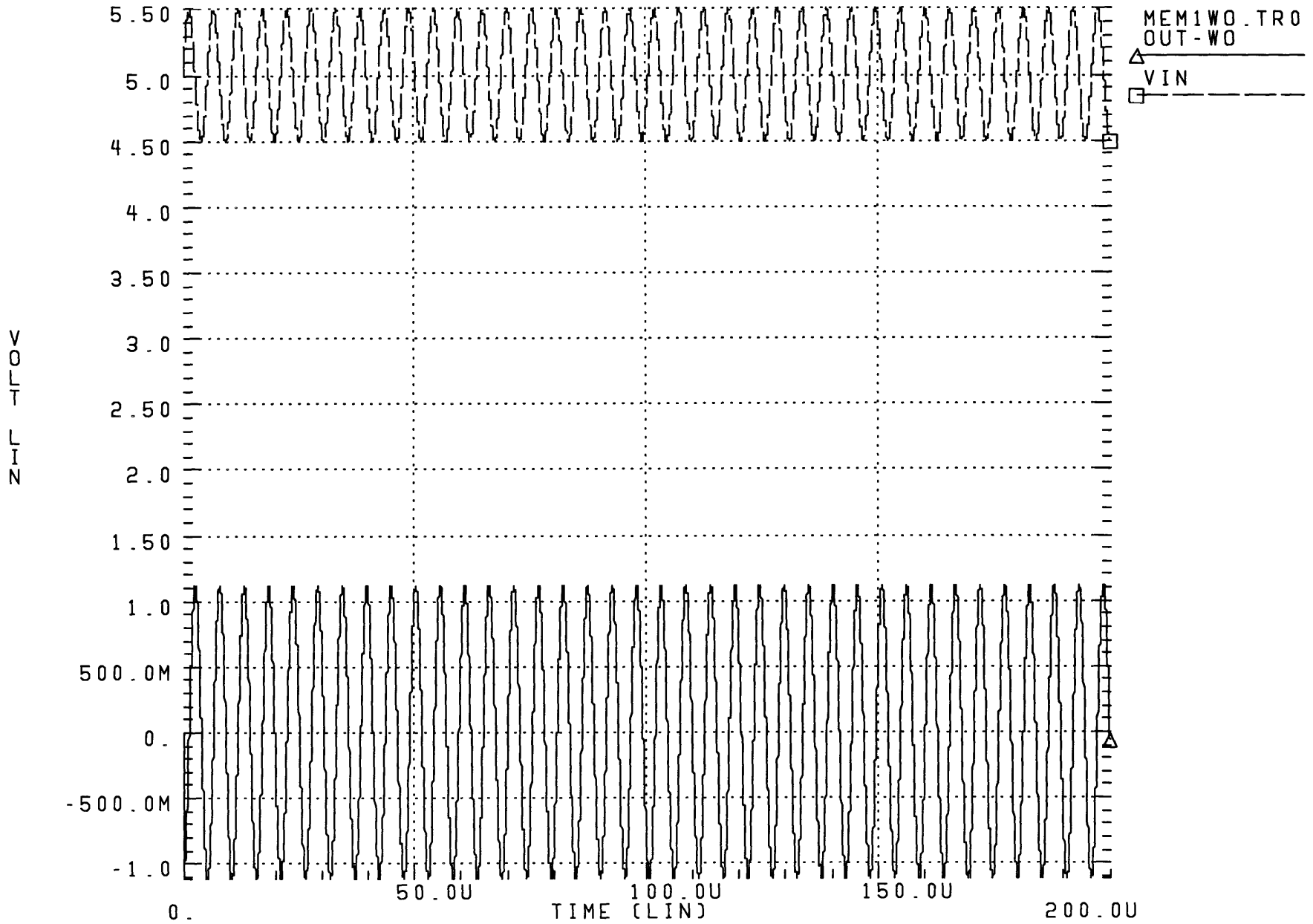

FIGURE 4-7: VOUT AND VIN OF THE WHOLE MEMS CIRCUIT VS. TIME, DRIVEN BY W
D-0.1WO.

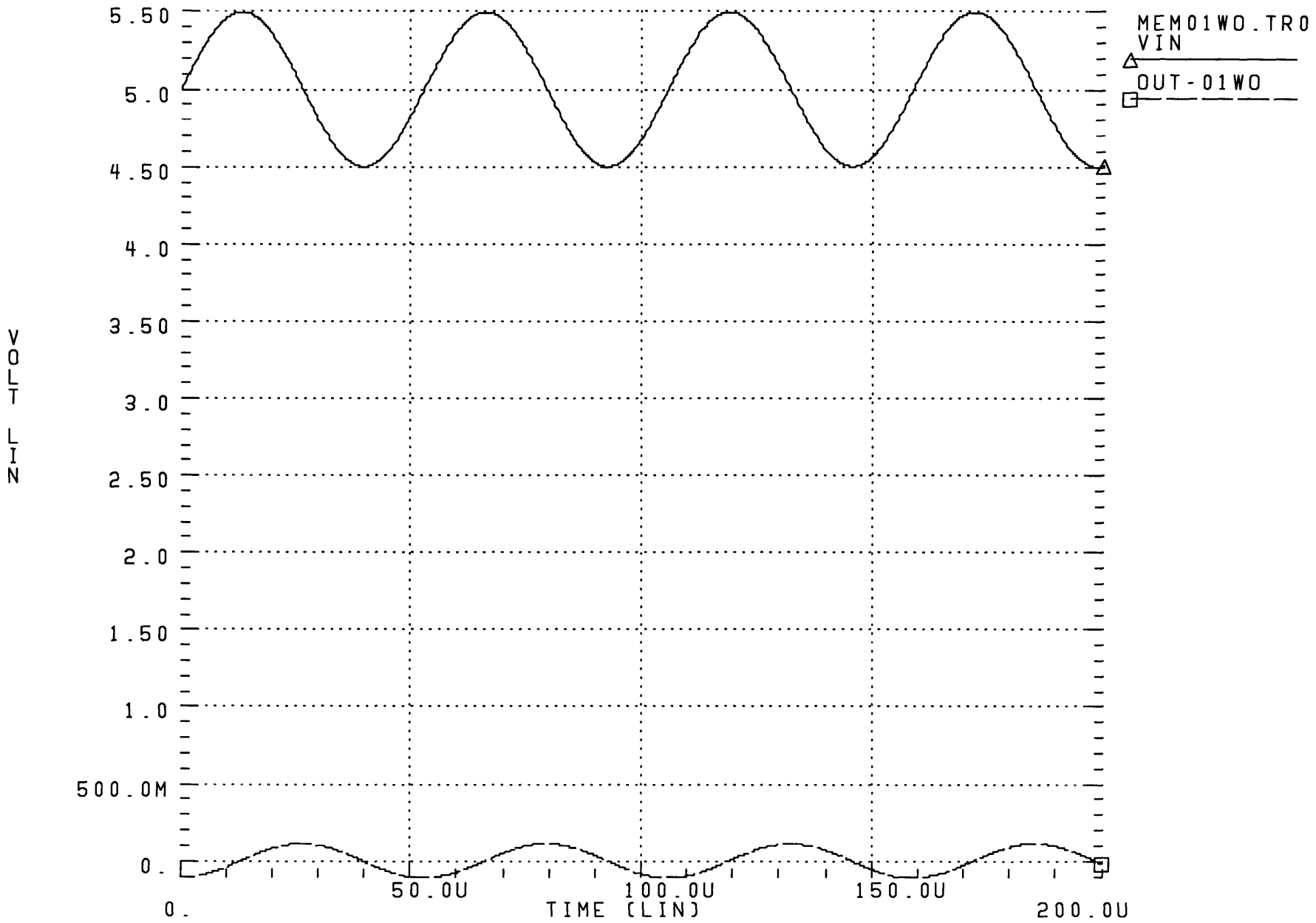

## 4.1 The Transfer Function Ratio of the MEMS Differentiator

A range of frequencies was used as a drive to the differentiator circuit and the corresponding AC outputs are recorded in Table 4.1. The output voltage $V_{OUT}$ along with both displacement voltages, $V_{XDC}$, and $V_{XAC}$ are also recorded in this table as well. For each entry, the ratio of $\left| \frac{V_{OUT}}{RCw_dV_{AC-in}} \right|$ is calculated. Listing Equation 3.13 once again, we have:

$$-V_{OUT} = RC_{MEMS}\frac{dV_{IN}}{dt} + RV_{IN}\frac{dC_{MEMS}}{dt} \tag{4.2}$$

$$-V_{OUT} = w_dRC_{MEMS}V_{AC}\cos w_dt + (V_{DC} + V_{AC}\sin w_dt)\left[\frac{RC_{MEMS}}{k\left(g_0 - \left(\frac{V_{XDC}+V_{XAC}}{k}\right)\right)}\left(\frac{dV_{XAC}}{dt}\right)\right] \tag{4.3}$$

If the MEMS capacitance were not a function of the input and the displacement but a constant capacitance instead, $\frac{dC_{MEMS}}{dt} = 0$ and $V_{OUT} = -w_dRC_{MEMS}V_{AC}\cos w_dt$. This makes the ratio of $\left| \frac{V_{OUT}}{RC_{MEMS}w_dV_{AC}} \right|$ =1. However, since $C_{MEMS}$ does depend on $V_{XAC}$ which varies with time and has a nonzero $\frac{dC_{MEMS}}{dt}$ value, the ratio of $\left| \frac{V_{OUT}}{RCw_dV_{AC}} \right|$ = 1+ $\xi$.

$$\left| \frac{-V_{OUT}}{RC_{MEMS}w_dV_{AC-in}} \right| = \left| \frac{w_dRC_{MEMS}V_{AC}\cos w_dt + (V_{DC} + V_{AC}\sin w_dt)\left[\frac{RC_{MEMS}}{k\left(g_0 - \left(\frac{V_{XDC}+V_{XAC}}{k}\right)\right)}\frac{dV_{XAC}}{dt}\right]}{w_dRC_{MEMS}V_{AC}} \right| \tag{4.4}$$

$$\left| \frac{V_{OUT}}{RC_{MEMS}w_dV_{AC-in}} \right| = 1 + \frac{V_{DC} + V_{AC}}{w_dkV_{AC}\left(g_0 - \left(\frac{V_{XDC}+V_{XAC}}{k}\right)\right)}\frac{dV_{XAC}}{dt} = 1 + \xi \tag{4.5}$$

where $\xi$ has the following value:

$$\xi = \frac{(V_{DC} + V_{AC})\left(\frac{dC_{MEMS}}{dt}\right)}{w_dC_{MEMS}V_{AC}} = \frac{V_{DC} + V_{AC}}{w_dkV_{AC}\left(g_0 - \left(\frac{V_{XDC}+V_{XAC}}{k}\right)\right)}\left(\frac{dV_{XAC}}{dt}\right) \tag{4.6}$$

This $\xi$ value is the output perturbation contributed by the mechanical motion of the capacitor plate set up by the AC drive used to measure the capacitance.

With $C_{MEMS}=\frac{\epsilon_o A}{\left(g_0-\left(\frac{V_{XDC}+V_{XAC}}{k}\right)\right)}$, when $V_{XAC} \ll V_{XDC}$, the value of $C_{MEMS}$ does not change significantly. Thus, $\frac{dC_{MEMS}}{dt}$ is very small; this makes the perturbation $\xi$ to be very small as well. However, when the circuit is driving at $w_o$, $V_{XAC} \sim V_{XDC}$ and $\xi$ is no longer insignificant. The transfer ratio of the circuit exceeds one and reaches the highest value for $\xi$. This highest value is due to the resonant effect of $V_{XAC}$. The results show that for most frequencies, the perturbation is under 2 % of tolerance, while at $w_o$, the perturbation goes up to 4.78%. The simulation demonstrates the MEMS capacitance with a maximum 4.78 % of tolerance caused to the perturbation generated by the AC component of the input voltage. The magnitude of $\left| \frac{-V_{OUT}}{RC_{MEMS}w_d V_{AC-in}} \right|$ is included in the Table 4.1. Figure 4-8 shows the graph of the ratio vs. a range of frequency both in the linear magnitude vs. linear frequency scale and linear magnitude vs. log frequency scale.

## 4.2 Conclusion

After measuring the ratio of the transfer function, one can conclude that the AC input does affect the MEMS capacitance, especially when the circuit is driven at the resonant frequency of the displacement RLC circuit. We can assume the MEMS capacitance measurement has a 4.78% tolerance due to the perturbation from the AC input. The various outputs of $V_{OUT}$, $V_{XDC}$ and $V_{XAC}$ are listed and compared. They all agree with the analytical results derived from Chapter 3. This project has accomplished the objective of obtaining the MEMS capacitance with a reasonable tolerance by separating the ouput of the DC component from the AC component perturbation.

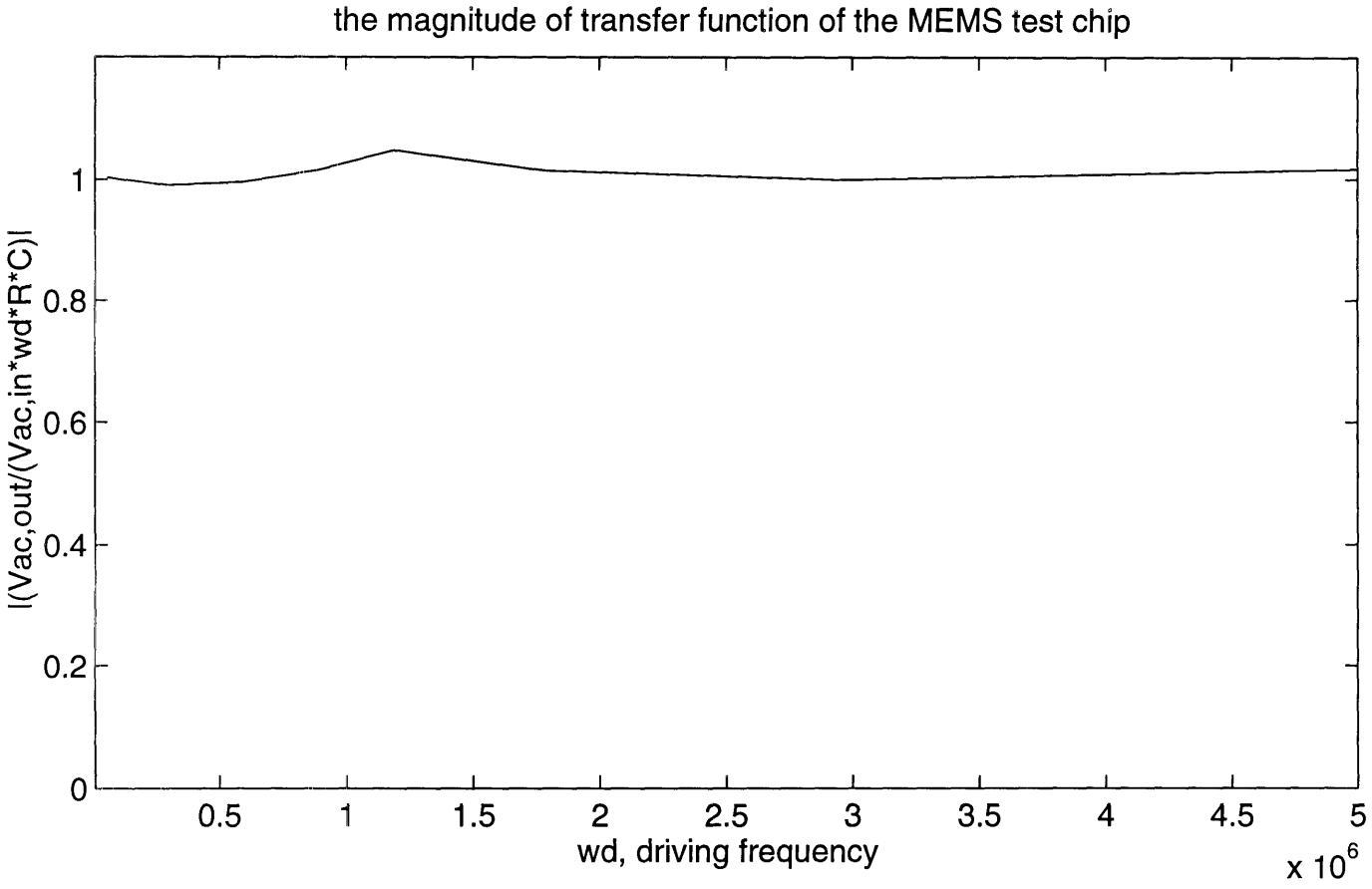
the magnitude of transfer function of the MEMS test chip
|(Vac,out/(Vac,in*wd*R*C)|
0
0.2
0.4
0.6
0.8
1
0.5
1
1.5
2
2.5
3
3.5
4
4.5
5
wd, driving frequency
x 10^6

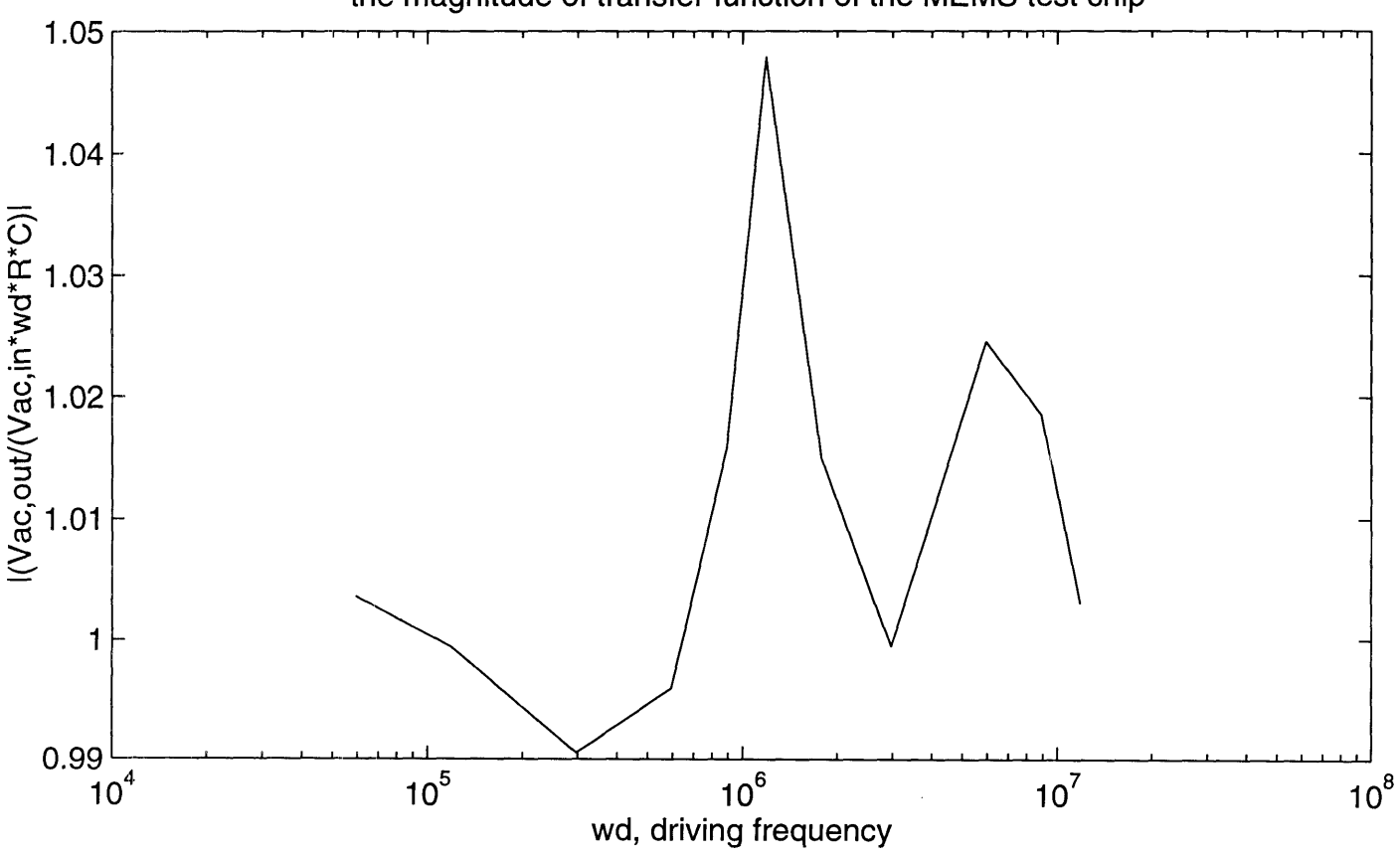
the magnitude of transfer function of the MEMS test chip
|(Vac,out/(Vac,in*wd*R*C)|
0.99
1
1.01
1.02
1.03
1.04
1.05
10^4
10^5
10^6
10^7
10^8
wd, driving frequency

| $w_d$ | $V_{AC-out}$ $(volts)$ | $\mid \frac{V_{AC-out}}{RCw_dV_{AC-in}} \mid$ | $V_{XDC}$ $(volts)$ | $V_{XAC}$ $(volts)$ |
|---|---|---|---|---|
| $0.05w_o$ | $56.03e-3$ | 1.003590123 | $2.2029e-6$ | $222.27e-9$ |
| $0.1w_o$ | $111.59e-3$ | 0.9993808836 | $2.2029e-6$ | $224.14e-9$ |
| $0.25w_o$ | $276.5e-3$ | 0.9905146135 | $2.2029e-6$ | $238.05e-9$ |
| $0.5w_o$ | $556.03e-3$ | 0.9959418455 | $2.2029e-6$ | $313.49e-9$ |
| $0.75w_o$ | $850.67e-3$ | 1.015793932 | $2.2029e-6$ | $486.75e-9$ |
| $w_o$ | 1.17 | 1.047831915 | $2.2029e-6$ | $2370e-9$ |
| $1.5w_o$ | 1.7 | 1.014993877 | $2.2029e-6$ | $163.91e-9$ |
| $2.5w_o$ | 2.79 | 0.9994704419 | $2.2029e-6$ | $40.79e-9$ |
| $5w_o$ | 5.72 | 1.024546701 | $2.2029e-6$ | $8.98e-9$ |
| $7.5w_o$ | 8.53 | 1.018576209 | $2.2029e-6$ | $3.86e-9$ |
| $10w_o$ | 11.20 | 1.003052773 | $2.2029e-6$ | $2.13e-9$ |

Table 4.1: Ratio of the MEMS Capacitance due to AC signal perturbation,$\mid \frac{V_{AC-out}}{RCw_dVAC-in} \mid$ vs. $w_d$.

# Appendix A

# HSPICE Simulation File

Below is the actual HSPICE input file used to simulate the MEMS characterization chip test chip. It consists of an ideal operational amplifier in the form of a voltage controlled voltage source, a resistor, a nonlinear functional capacitor described by equation 1-2, and the two displacement RLC circuits, with their input external force as a dependent voltage sources; the dependent sources depend on both the input voltage of the whole circuit as well as their own displacement voltages. In this example, it is driven at a frequency equal to the resonant frequency of the RLC displacement circuit.

```
----------HSPICE INPUT FILE ----------
The macromodel simulation of the mems materials characterization test chip
.param ep=8.85e-12 vdc=5 vac=.5 g0=1.6e-6 area=2.5e-8 k=164 b=1e-10 m=1.1655e-
10 pi=3.1415926535
.param g0k='g0 * k' w0 = 'sqrt((k/m)-((b**2)/(2*(m**2))))' fd='1 *w0/(2*pi)'
.param fconst='((ep*area*(vdc**2+.5*vac**2))/(g0**2))'
.param fcon2='.5*ep*area/(g0**2)'
.param p0='-.5*(vac**2)*fcon2' p1='2*vdc*fcon2' p2='-1*fcon2*(vac**2)/g0k'
.param p3='fcon2' p4='4*vdc/g0k*fcon2' p5='-1.5*(vac**2)/(g0k**2)*fcon2'
.param p6=0 p7='2*fcon2/g0k' p8='6*vdc*fcon2/(g0k**2)' p9=0 p10=0 p11=0
.param p12='3*fcon2/(g0k**2)' p13=0 p14=0
v1 1 0 vdc
```

```
v2 2 1 sin (0 vac fd 0 0 0)
c1 2 3 c='((ep*area)/(g0-(v(vxdc)+v(vxac))/k))'
r1 3 out 1.35e7
e1 out 0 poly(1) 3 0 0 1e5
e2 4 0 poly(1) vxdc 0 fconst '(2*fconst/g0k)' '((3*fconst)/(g0k**2))' '(4*fconst/g0k**3)'
rdc 4 vxdc b
cdc vxdc 0 '1/k'
e3 5 0 poly(2) 2 1 vxac 0 p0 p1 p2 p3 p4 p5 p6 p7 p8 p9 p10 p11 p12 p13 p14
lac 5 6 m
rac 6 vxac b
cac vxac 0 '1/k'
*.tran 100n 305u
.tran 10n 150u
.plot tran v(out)
*.ac dec 10 1k 1591.54931
.option post imax=40 ft=0.1
.end
```

THE END

# Bibliography

[1] K. Petersen J. Bryzek. Micromachines: Advances in performance, fabrication techniques. *IEEE Spectrum*, pages 20–31, May 1994.

[2] J.R. Gilbert P.M. Osterberg, R.Gupta and S.B. Senturia. Quantitative emodels for the measurement of residual stress, poisson's ratio and young's modulus using electrostatic pull-in of beams and diaphragms. *Solid-State Sensor and Actuator Workshop*, pages 184–188, June 1994.

[3] *HSPICE User's Manual*, volume 2. Meta-Software, second edition, 1992.